Synthesis of a Large, Shape-Flexible, Solvatomorphic Porous Organic Cage

Baiyang Teng,[†] Marc A. Little[*,†] Tom Hasell,[†] Samantha Y. Chong,[†] Kim E. Jelfs,[‡] Michael E. Briggs,[†] and Andrew I. Cooper[*,†]

[†]Department of Chemistry and Materials Innovation Factory, University of Liverpool, Liverpool, L69 7ZD, U.K.

[‡]Department of Chemistry, Imperial College London, Molecular Sciences Research Hub, White City Campus, Wood Lane, W12 0BZ, U.K.

Electronic Supporting Information

Materials: 2-Hydroxy-1,3,5-benzenetricarbaldehyde and *cis*-1,3-cyclohexanediamine were purchased from TCI, 1,3,5-triformylbenzene was purchased from Manchester Organics. Solvents were reagent or HPLC grade and were purchased from Fisher Scientific. All chemicals were used as received.

NMR: ^{1}H and ^{13}C spectra were recorded using an internal deuterium lock for the residual protons in $CDCl_3$ (δ = 7.26 ppm) at ambient probe temperature on a Bruker Avance 400 MHz NMR spectrometer.

Diffusion NMR: All measurements were carried out non-spinning on a 400 MHz Bruker Avance 400 spectrometer, using a 5 mm indirect detection probe, equipped with a z-gradient coil producing a nominal maximum gradient of 34 G cm^{-1}. Diffusion data was collected using the Bruker double stimulated emission gradient pulse sequence (dstegp3s) to minimise the effect of convection in $CDCl_3$. A diffusion encoding pulse δ of length 3 – 4 ms, and diffusion delay Δ of 0.14 – 0.15 s were used. Gradient amplitudes were equally spaced between 1.70 to 32.4 G cm^{-1}. Each FID was acquired using 16 k data points. All experiments were carried out at a nominal probe temperature of 298 K, with an air flow of 800 m^3 min^{-1} to minimise convection. ^{1}H NMR Spectra were recorded using an internal deuterium lock for the residual protons in $CDCl_3$ (δ 7.26).

Hydrodynamic radii, R_S, of solution-phase species were calculated from the Stokes-Einstein equation assuming molecules have a spherical geometry:

$$D = \frac{kT}{6\pi\eta R_h}$$

Where kT is the thermal energy and η is the viscosity of the solvent. Viscosities were assumed to be that of the native solvent (in the case of $CDCl_3$ at 298 K, this was 0.542 cP).

HRMS: High resolution mass spectrometry was carried out using an Agilent Technologies 6530B accurate-mass QTOF Dual ESI mass spectrometer (capillary voltage 4000 V, fragmentor 225 V) in positive-ion detection mode. The mobile phase was MeOH + 0.1% formic acid at a flow rate of 0.25 mL/min.

TGA: Thermogravimetric analysis was carried out using a Q5000IR analyser (TA Instruments) with an automated vertical overhead thermobalance.

PXRD: Laboratory powder X-ray diffraction data were collected in transmission mode on samples held on thin Mylar film in aluminium well plates on a Panalytical X'Pert PRO MPD equipped with a high throughput screening XYZ stage, X-ray focusing mirror and PIXcel detector, using Ni filtered Cu-Kα radiation. PXRD data from samples contained in borosilicate glass capillaries were collected in transmission geometry on a Panalytical Empyrean diffractometer producing Cu-Kα radiation and equipped with an X-ray focusing mirror. Data were collected using a PIXcel 3D detector in 1D scanning mode and samples were spun to improve powder averaging.

SEM: Scanning electron microscopy images were obtained using a Hitachi S-4800 cold Field Emission Scanning Electron Microscope (FE-SEM). Scanning-mode samples were prepared by depositing dry crystals on 15 mm Hitachi M4 aluminium subs using an adhesive high-purity carbon tab before coating with a 2 nm layer of gold using an Emitech K550X automated sputter coater. Imaging was conducted at a working distance of 8 mm and a working voltage of 3 kV using a mix of upper and lower secondary electron detectors. The FE-SEM measurement scale bar was calibrated using certified SIRA calibration standards.

Computational modelling: This was carried out at the forcefield level using the OPLS all atom forcefield[1] in MacroModel (version 10.3.015, Schrödinger, LLC, New York, NY, 2015-3), which we have previously found to produce reliable structures for different conformations of porous organic cages.[2] The two molecular geometries of the cage were taken from the single crystal XRD structure, and the OH groups were added randomly, one on each arene ring. The structures were then geometry optimised with the Polak-Ribier Conjugate Gradient method and a convergence criteria of 0.05 kJ mol^{-1} $Å^{-1}$ and both conformations ended up in the same energy minimum. To investigate the conformational energy landscape further and to see if there were other stable conformations, we conducted a conformer search. The search used the low-mode search method, which is based on eigenvector following. The number of steps (starting from a minimum of 20000) was increased until convergence was reached, *i.e.*, the number of low energy conformers found was constant despite an additional 5000 steps being carried out. The energy window for saved conformers was set to 25 kJ mol^{-1} and the minimum and maximum moves as 3 Å and 10 Å, respectively.

Gas Sorption Analysis: BET surface areas were measured by nitrogen sorption at 77.3 K. Gas sorption isotherms for N_2, H_2, CO_2, Xe, and Kr were measured using Micromeritics 3flex, 2020, or 2420 volumetric adsorption analysers at the temperatures specified on the gas sorption plots.

Single crystal XRD: Single crystal X-ray data sets were measured on a Bruker D8 Venture Advance diffractometer equipped with IμS microfocus source (Cu-Kα radiation, λ = 1.54185 Å, Kappa 4-circle goniometer, PHOTON100 CMOS detector); at beamline 11.3.1, Advanced Light Source, Berkeley, USA, using silicon monochromated synchrotron radiation (λ = 0.7749 Å, PHOTON100 CMOS detector); or at beamline I19, Diamond Light Source, Didcot, UK using silicon double crystal monochromated synchrotron radiation (λ = 0.6889 Å, Rigaku Saturn724+ detector). Unless started solvated single crystals, isolated from the crystallization solvent mixture, were covered with protective oil, mounted on a MiTeGen loop, and flash cooled to 100 K under a dry nitrogen gas flow. Rigaku frames were converted to Bruker compatible frames using the programme ECLIPSE.[3] Empirical absorption corrections, using the multi-scan method, were performed with the program SADABS.[4,5] Structures were solved with by direct methods using SHELXD,[6] SHELXT,[7] or by direct methods using SHELXS,[8] and refined by full-matrix least squares on $|F|^2$ by SHELXL,[9] interfaced through the programme OLEX2.[10] Unless stated all non-H-atoms were refined anisotropically, and H-atoms were fixed in geometrically estimated positions and refined using the riding model. Supplementary single crystal XRD data, including structure factors, is available free of charge from the Cambridge Crystallographic Data Centre (CCDC) via www.ccdc.cam.ac.uk/data_request/cif. For full refinement details, see **Table S1-S2** and supporting CIF files.

Table S1. Refinement details for 2(**CC20**)·46(CH_2Cl_2)·46(CH_4O) and (**CC20**)·32(C_5H_{12}).

Sample Reference	2(**CC20**)·46(CH_2Cl_2)·46(CH_4O)[a]	(**CC20**)·32(C_5H_{12})[a]
Collection Temperature	100 K	100 K
λ [Å]	Cu-Kα	0.6889
Formula	$C_{380}H_{612}Cl_{92}N_{48}O_{62}$	$C_{304}H_{528}N_{24}O_8$
Mr	10106.54	4647.47
Crystal Size (mm)	0.15 x 0.15 x 0.12	0.15 x 0.15 x 0.11
Crystal System	Cubic	Cubic
Space Group	$Pm\bar{3}$	$Im\bar{3}$
a [Å]	24.880(5)	24.829(7)
V [Å^3]	15402(9)	15306(13)
Z	1	2
D_{calcd} [g cm^{-3}]	1.071	1.008
μ [mm^{-1}]	4.002	0.056
F(000)	5198	5168
2θ range [°]	2.511–33.361	1.124–15.348
Reflections collected	4605	10577
Independent reflections, R_{int}	1116, 0.0295	687, 0.0435
Obs. Data [I > 2σ]	745	491
Data / restraints / parameters	1116 / 98 / 152	687 / 53 / 76
Final R1 values (I > 2σ(I))	0.1462	0.1350
Final *R*1 values (all data)	0.1631	0.1464
Final *wR*(F^2) values (all data)	0.3675	0.4338
Goodness-of-fit on F^2	2.617	3.281
Largest diff. peak and hole [e.A^{-3}]	0.257 / -0.426	0.195 / -0.331
CCDC	1881384	1881385

[a] The SQUEEZE routine was used to mask disordered solvent molecules during the final refinement cycles.

Table S1 continued. Refinement details for 2(**CC20**)·26($CHCl_3$)·23(C_2H_3N) and 2(**CC20**)·17.5(C_5H_{12}).

Sample Reference	2(**CC20**)·26($CHCl_3$)·23(C_2H_3N)[a]	2(**CC20**)·17.5(C_5H_{12})[a]
Collection Temperature	100 K	100 K
λ [Å]	0.6889	0.7749
Formula	$C_{360}H_{407}Cl_{78}N_{71}O_{16}$	$C_{375.50}H_{546}N_{48}O_{16}$
Mr	8749.64	5988.57
Crystal Size (mm)	0.21 x 0.14 x 0.09	0.14 x 0.09 x 0.08
Crystal System	Triclinic	Triclinic
Space Group	$P\bar{1}$	$P\bar{1}$
a [Å]	19.050(5)	19.0938(7)
b [Å]	22.376(6)	22.1025(8)
c [Å]	33.050(9)	29.1723(11)
α [°]	79.525(3)	84.794(2)
β [°]	86.993(3)	85.553(2)
γ [°]	66.012(2)	67.059(2)
V [Å^3]	12653(6)	11278.9(7)
Z	1	1
D_{calcd} [g cm^{-3}]	1.148	0.882
μ [mm^{-1}]	0.423	0.064
F(000)	4518	3263
2θ range [°]	0.981–18.248	2.061–20.623
Reflections collected	74249	47395
Independent reflections, R_{int}	19877, 0.0479	17700, 0.0499
Obs. Data [I > 2σ]	14921	10887
Data / restraints / parameters	19877 / 1545 / 1822	17700 / 1562 / 1681
Final R1 values (I > 2σ(I))	0.1311	0.0979
Final *R*1 values (all data)	0.1478	0.1319
Final *wR*(F^2) values (all data)	0.3680	0.2925
Goodness-of-fit on F^2	2.387	1.639
Largest diff. peak and hole [e.A^{-3}]	0.500 / -0.433	0.464 / -0.267
CCDC	1881386	1881387

[a] The SQUEEZE routine was used to mask disordered solvent molecules during the final refinement cycles.

Synthesis of **CC20**

A solution of methanol/dichloromethane (1:1 v/v, 350 mL) was slowly added onto solid 2-hydroxy-1,3,5-triformylbenzene (449 mg, 2.52 mmol) without stirring at room temperature. Trifluoroacetic acid (10 μL) was added directly to this suspension followed by a solution of *cis*-1,3-cyclohexanediamine (432 mg, 3.78 mmol) dissolved in methanol/dichloromethane (1:1 v/v, 50 mL). The unstirred reaction was sealed and left to stand. Over a period of 14 days all of the solid 2-hydroxy-1,3,5-triformylbenzene was consumed, and crystals grew on the inner sides of the round bottom flask. The yellow solution was gradually exchanged with *n*-pentane then the crystals were soaked in *n*-pentane for a further 7 days. The solvent was carefully decanted and the crystals were dried under a flow of nitrogen gas for 7 days then under vacuum for a further 7 days at ambient temperature to afford an orange solid (435 mg, 58%). ^{1}H NMR ($CDCl_3$): δ 14.70–14.20 (m, O*H*, 8H), 8.79 (s, C*H*=N, 8H), 8.41 (m, C*H*=N, 8H), 8.24 (s, C*H*=N, 8H), 8.06 (m, Ar*H*, 16H), 3.44–3.18 (m, C*H*N, 24H), 2.1–1.36 (m, CH_2, 96H); ^{13}C NMR ($CDCl_3$): 162.8, 158.0, 153.70, 132.2, 131.2, 127.0, 123.7, 119.6, 69.6, 68.0, 42.6, 33.3, 22.9, 22.6; MS (HRMS)$^{+}$ calcd for $C_{144}H_{168}N_{24}O_8$ $[M+2H]^{2+}$: 1181.6811; found 1181.6881.

Note: Each aromatic ring in the cage contains a single hydroxyl group that is disordered throughout the structure. This results in the formation of a large number of regioisomers that complicates the NMR.

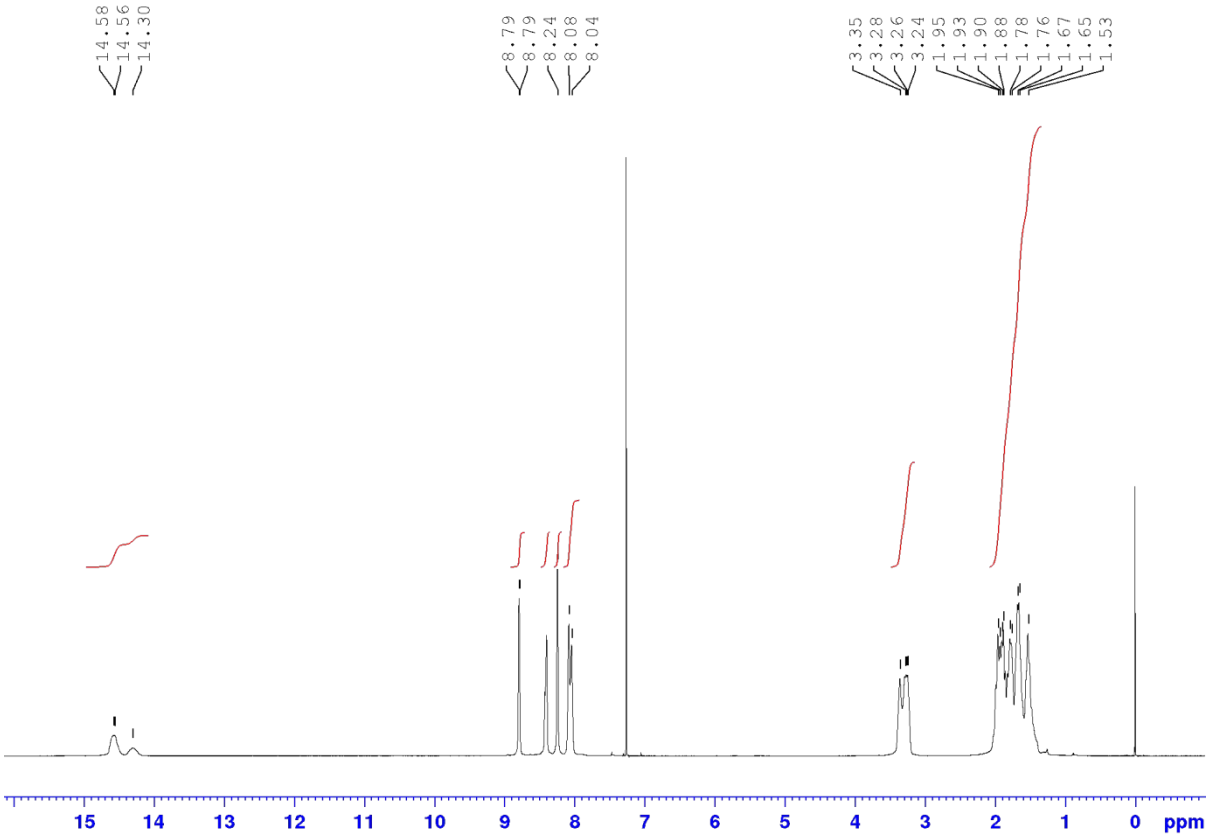

Figure S1. ^{1}H NMR (400 MHz) for cage **CC20** in $CDCl_3$.

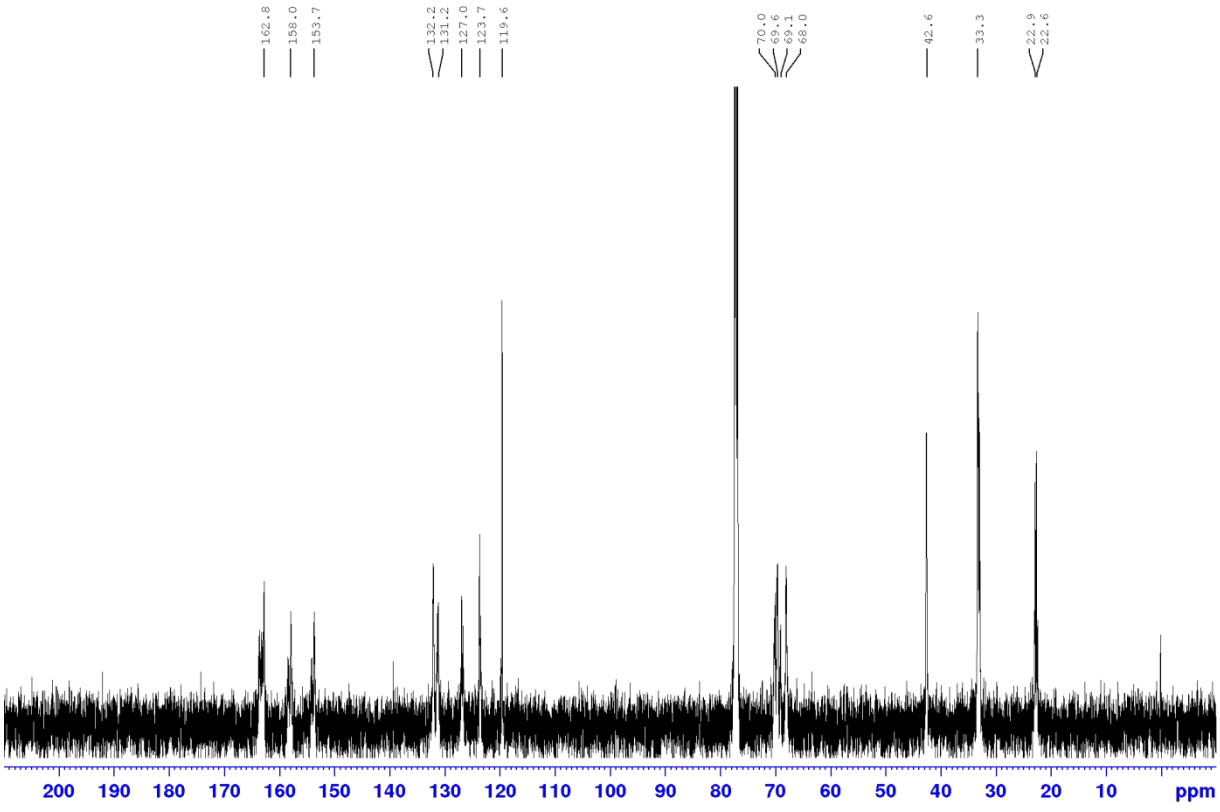

Figure S2. ^{13}C NMR (100 MHz) for cage **CC20** in $CDCl_3$.

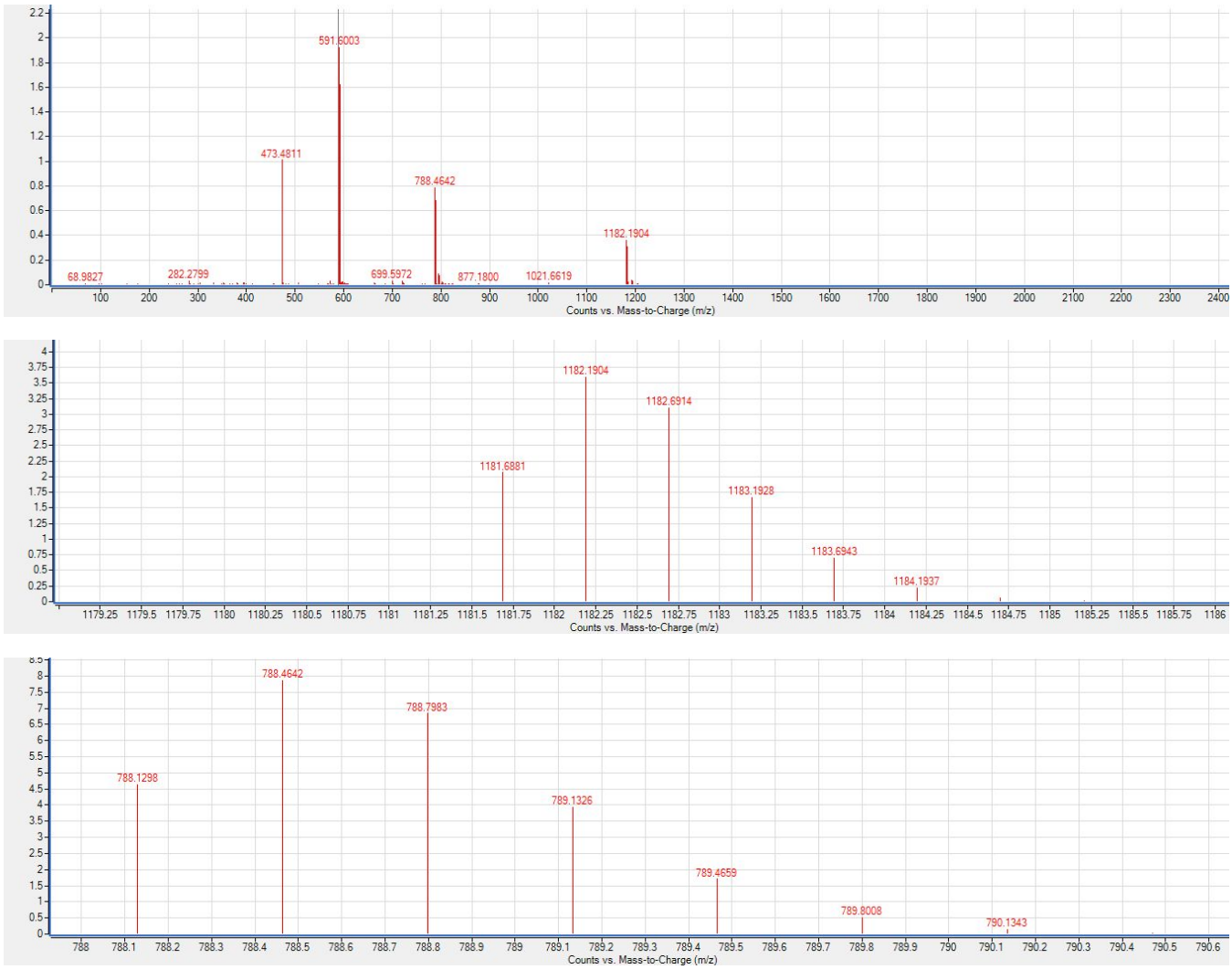

Figure S3. High resolution mass spectrometry of **CC20**.

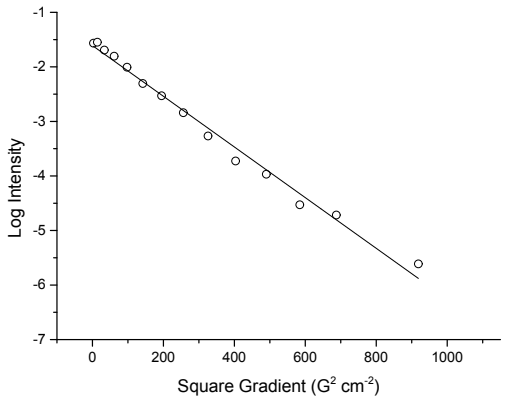

A diffusion coefficient of 3.65×10^{-10} m^2 s^{-1} was measured, this is consistent with a molecular cage approximately 2.2 nm in diameter.

Figure S4. DOSY NMR for **CC20** in $CDCl_3$

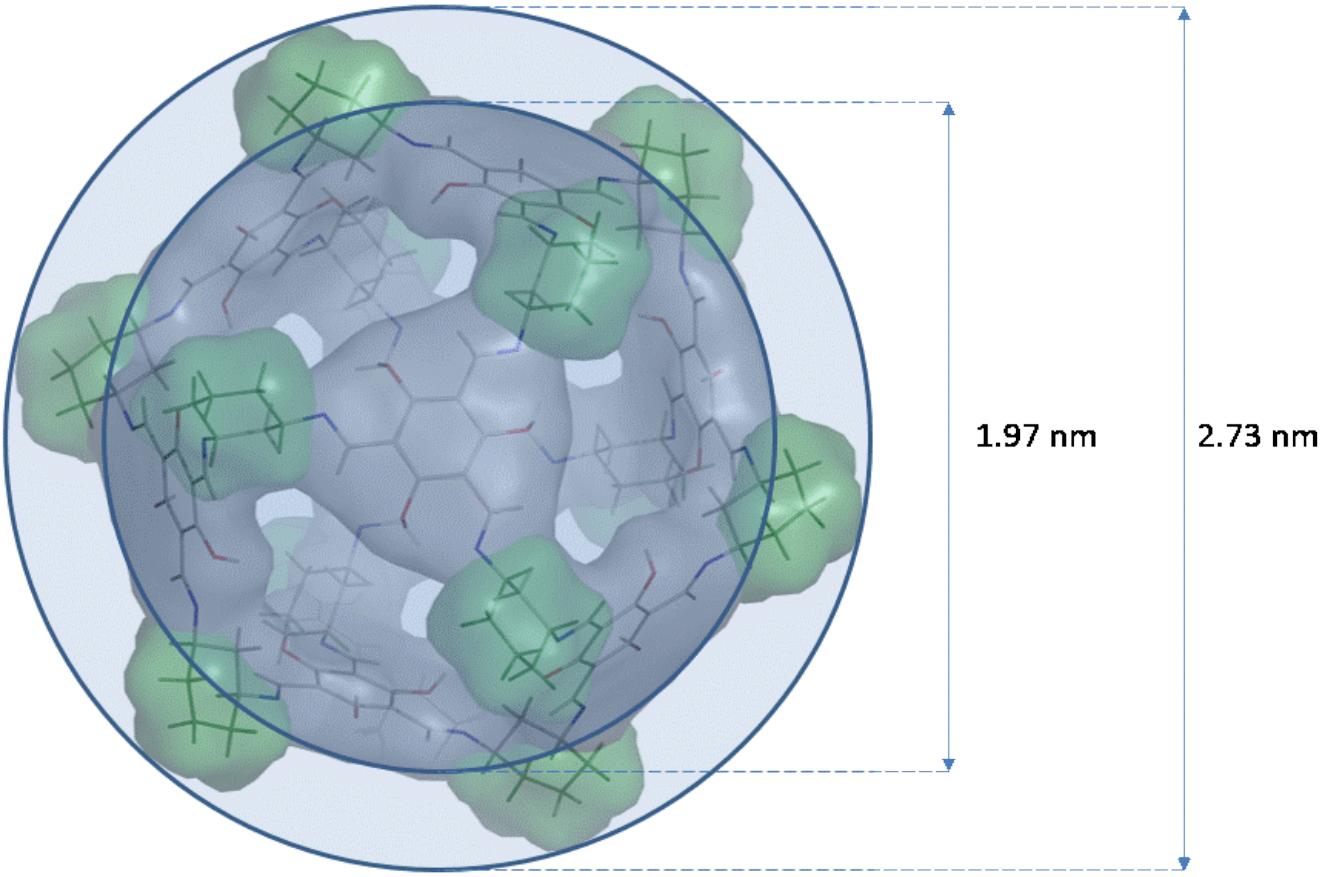

Figure S5. Calculated minimum and maximum diameters of **CC20**.

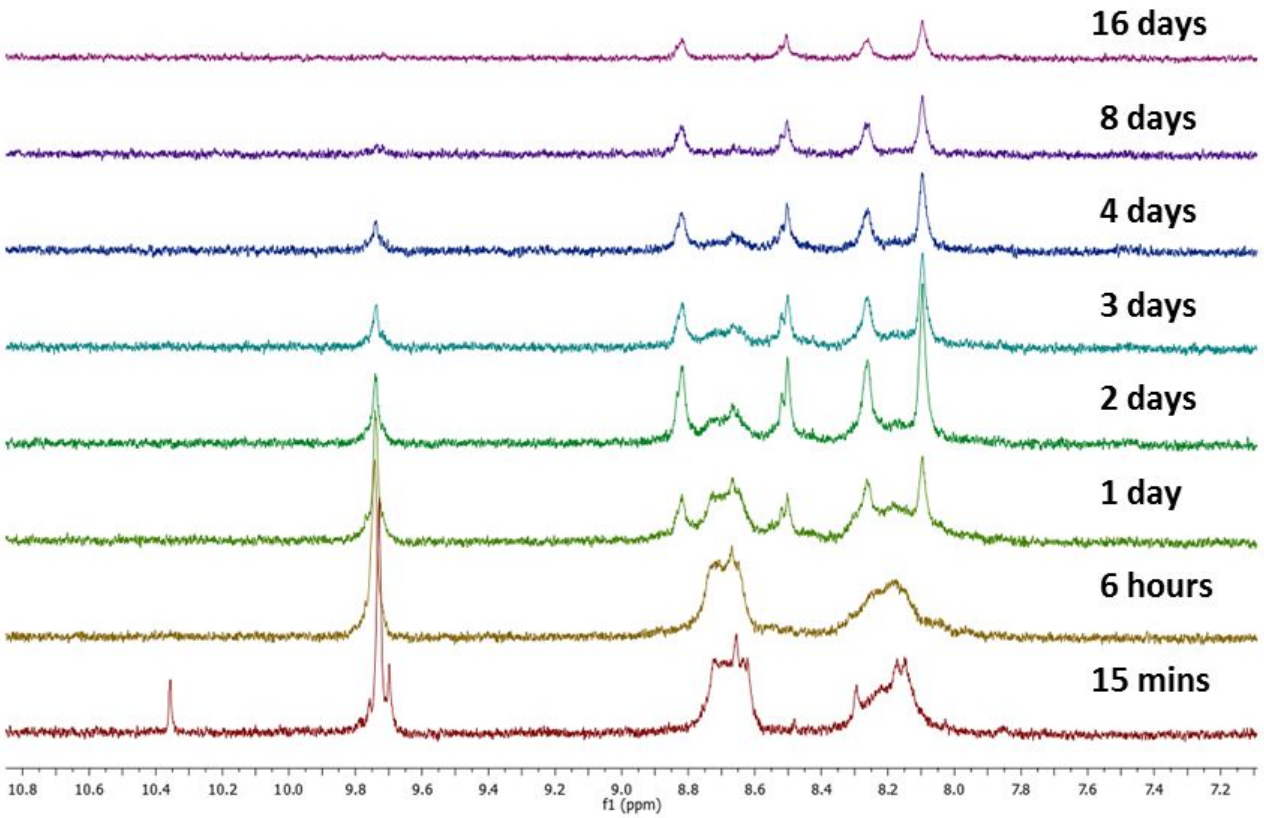

Figure S6. In-situ ^{1}H-NMR (400 MHz) monitoring of **CC20** formation in d_2-DCM/d_3-MeOH. The intensity of the signals decreases with time due to crystallization of the cage in the NMR tube.

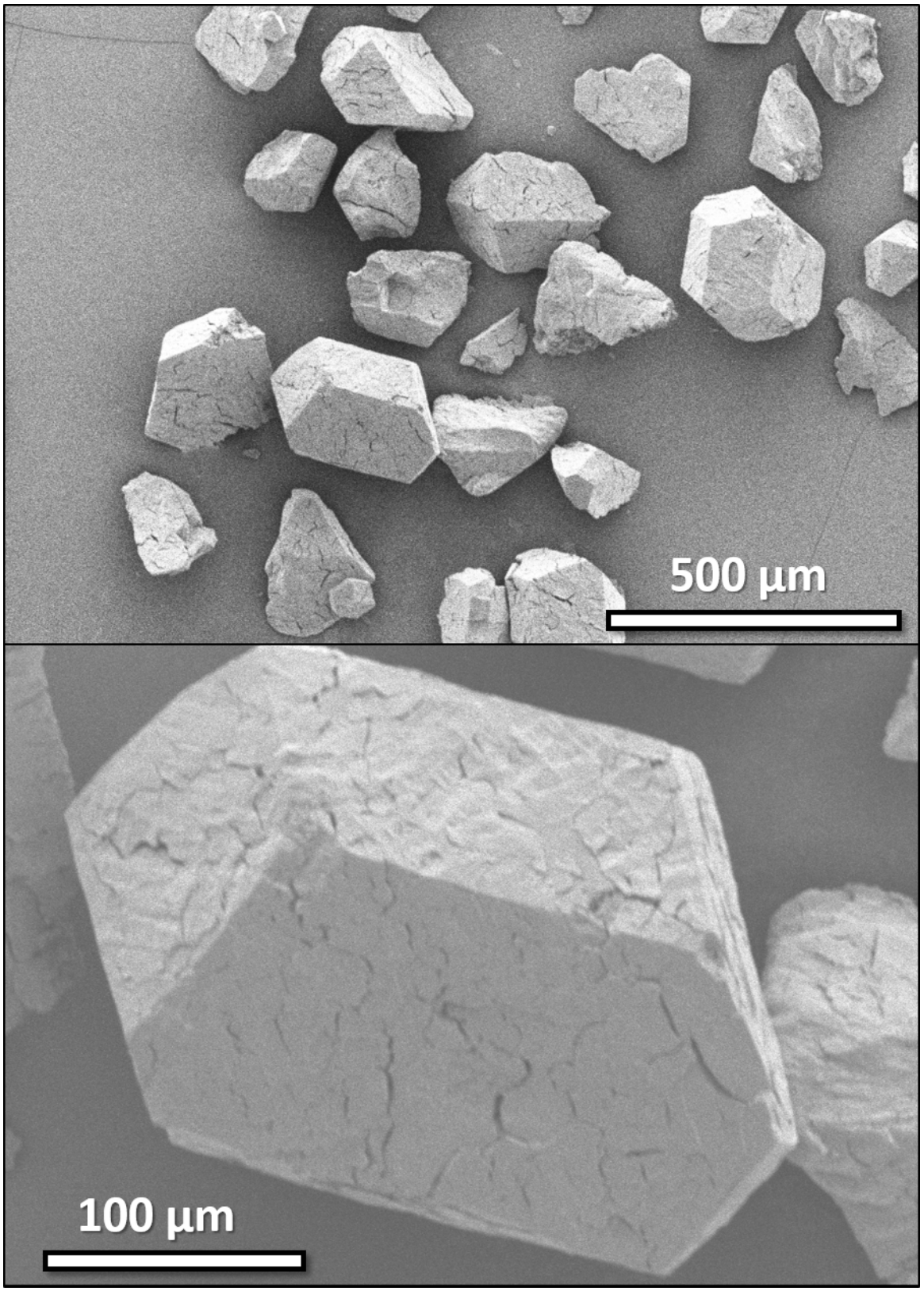

Figure S7. SEM micrographs of the as synthesized *P*m$\bar{3}$ DCM/methanol solvate of **CC20.**

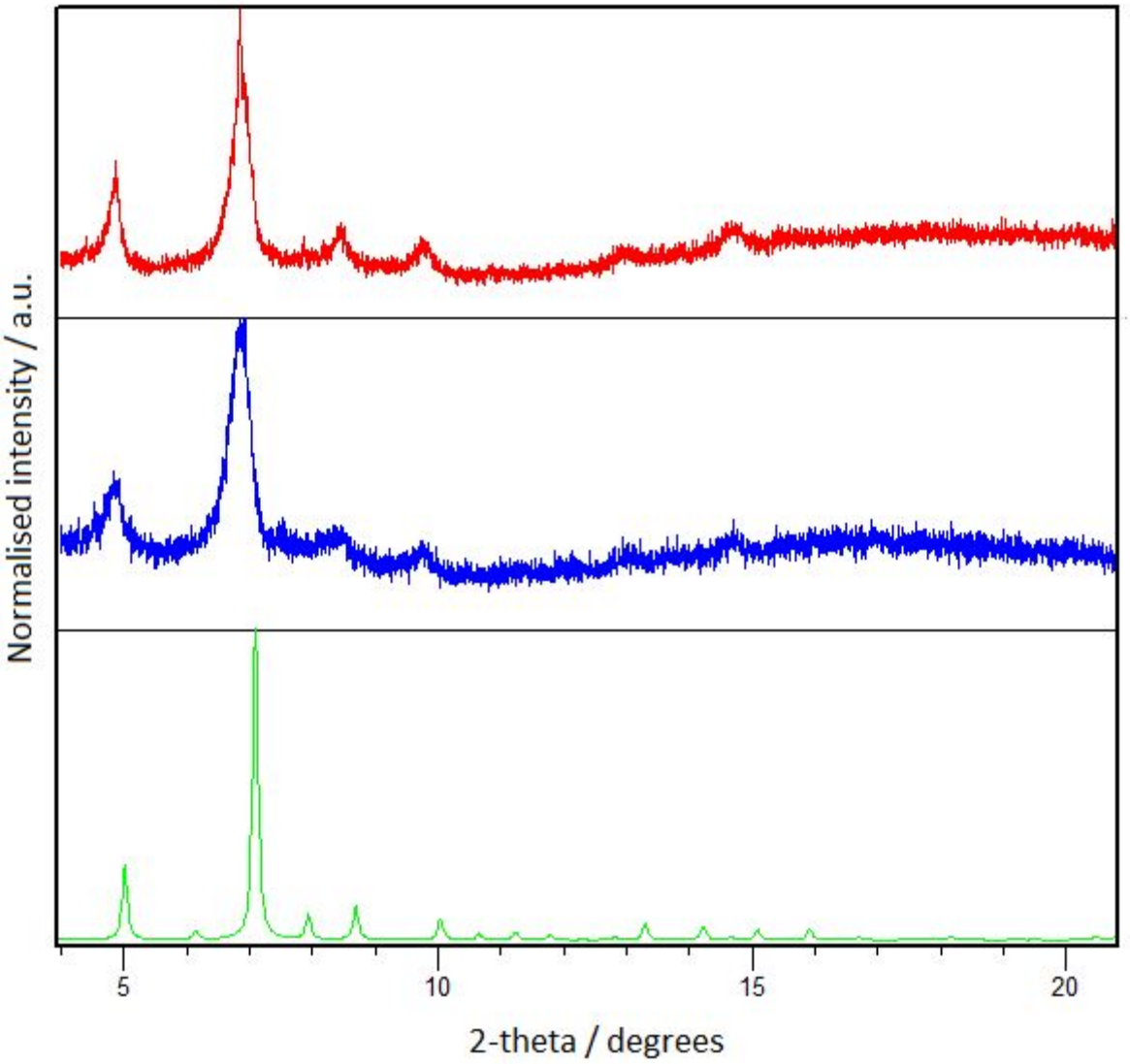

Figure S8. Simulated PXRD pattern of the DCM/MeOH *P*m$\bar{3}$ solvate (green, bottom), shown below the PXRD patterns recorded after drying the DCM/MeOH solvated **CC20** material in air (red, top), and under vacuum at 30 °C (blue, middle).

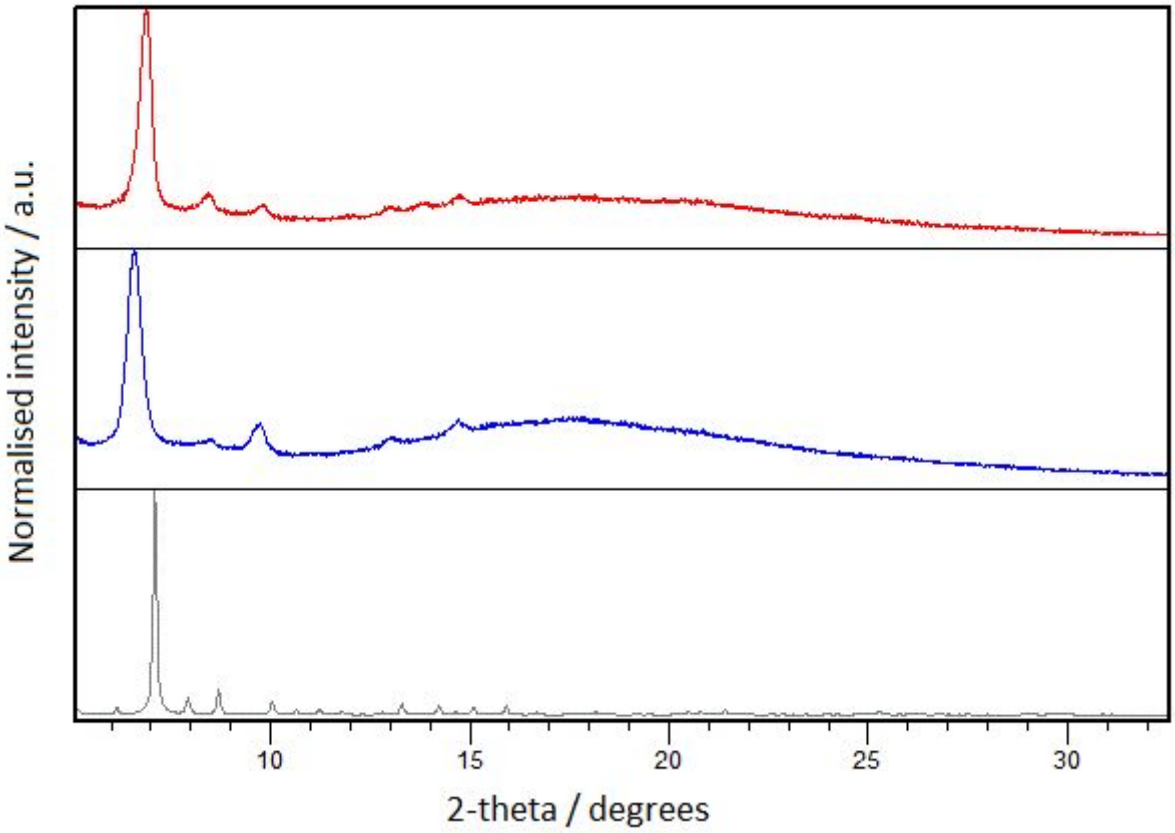

Figure S9. Simulated PXRD pattern of the DCM/MeOH *P*m$\bar{3}$ solvate (black, bottom), shown below the PXRD patterns recorded after desolvation of the DCM/MeOH solvated material at 90 °C under vacuum (red, top), and after gas sorption (blue, middle).

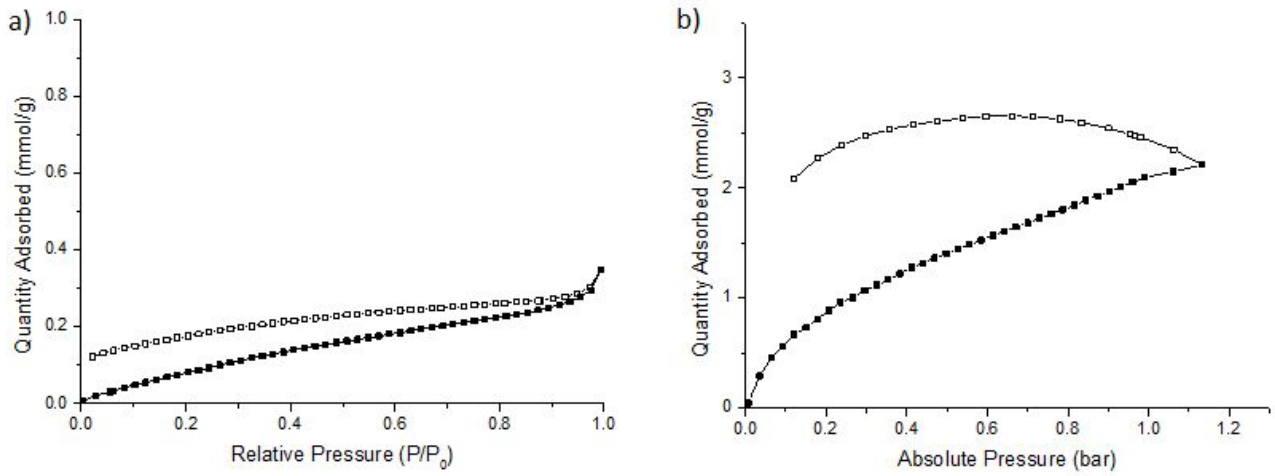

Figure S10. Gas sorption isotherms for the DCM/MeOH prepared **CC20** material, recorded after degassing the sample for 15 hours at 90 °C. a) N_2 sorption isotherms recorded at 77.3 K, and b) H_2 sorption isotherm at 77.3 K (closed symbols for adsorption, open for desorption). The severe hysteresis in the desorption isotherm of hydrogen, including a slight increase in uptake during the desorption cycle, is due to slow kinetics. This effect is likely caused by the low crystallinity of the material (Figure. S10) creating convoluted diffusion pathways.

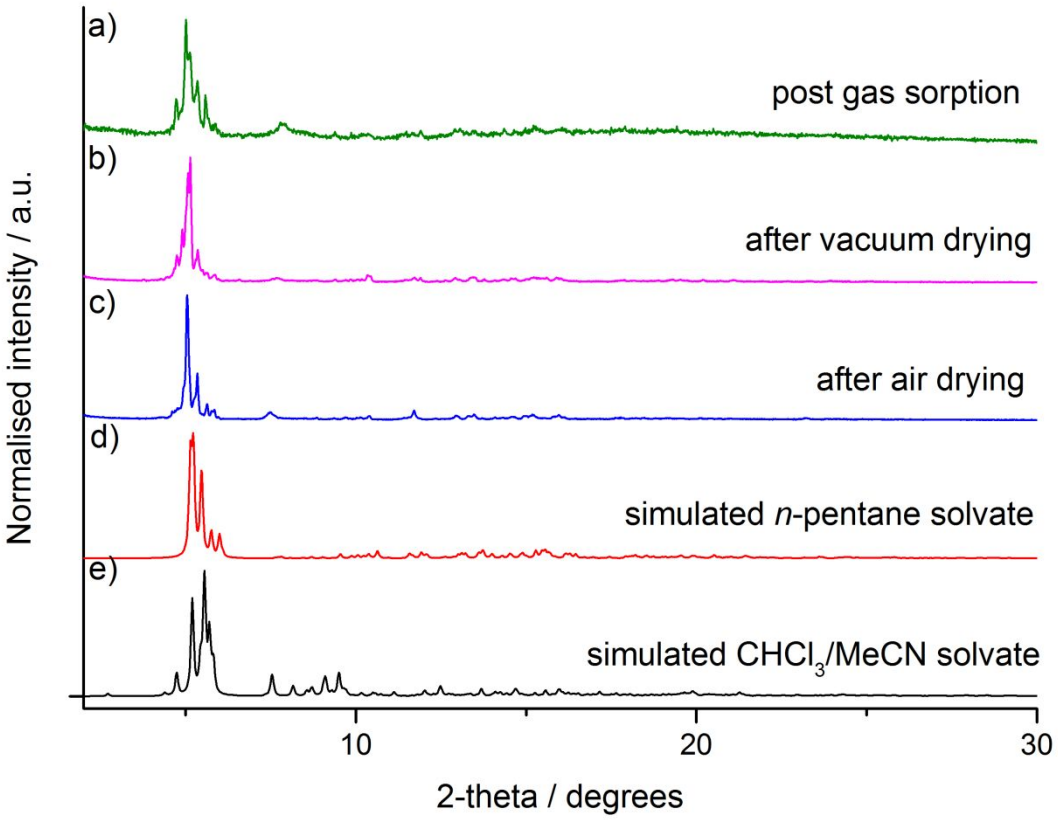

Figure S11. PXRD patterns recorded after activating the *n*-pentane solvated $Im\bar{3}$ **CC20** phase and recording gas sorption isotherms. PXRD patterns recorded; (a) post gas sorption analysis; (b) after drying the *n*-pentane solvated crystals under dynamic vacuum at ambient temperature; and (c) after drying the *n*-pentane solvated crystals in air at ambient temperature. Simulated PXRD patterns of the *n*-pentane $Im\bar{3}$ (d) and CH_2Cl_2/MeOH $Pm\bar{3}$ (e) **CC20** solvates.

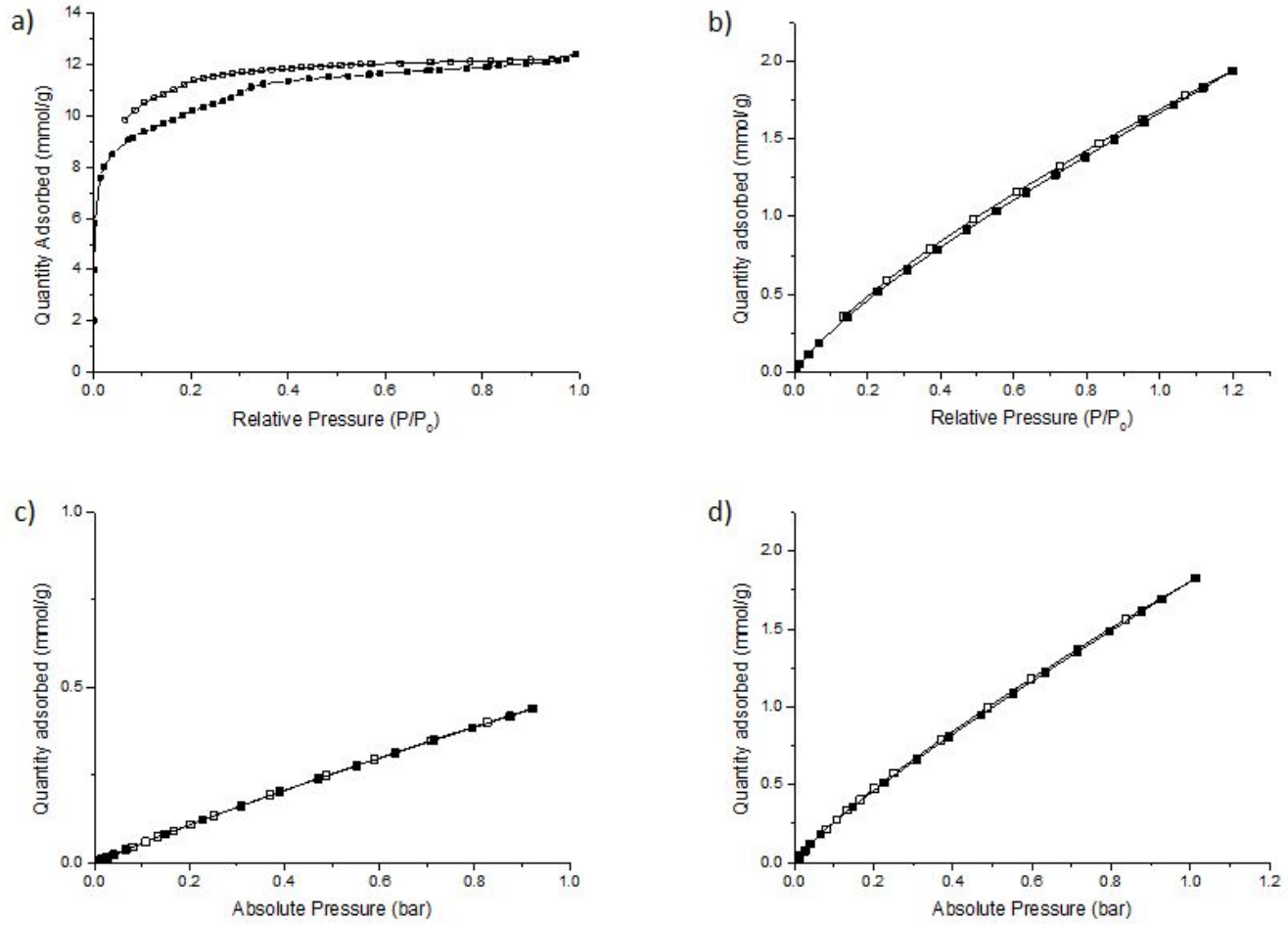

Figure S12. Gas sorption isotherms recorded for the **CC20** material that was initially crystallised from CH_2Cl_2/MeOH, then solvent exchanged with *n*-pentane, before being degassed for 30 hours under vacuum at 30 °C. a) N_2 sorption isotherms recorded at 77.3 K, b) CO_2 sorption isotherm at 273 K, c) Kr sorption isotherm at 273 K, and d) Xe sorption isotherm at 273 K (closed symbols for adsorption, open for desorption).

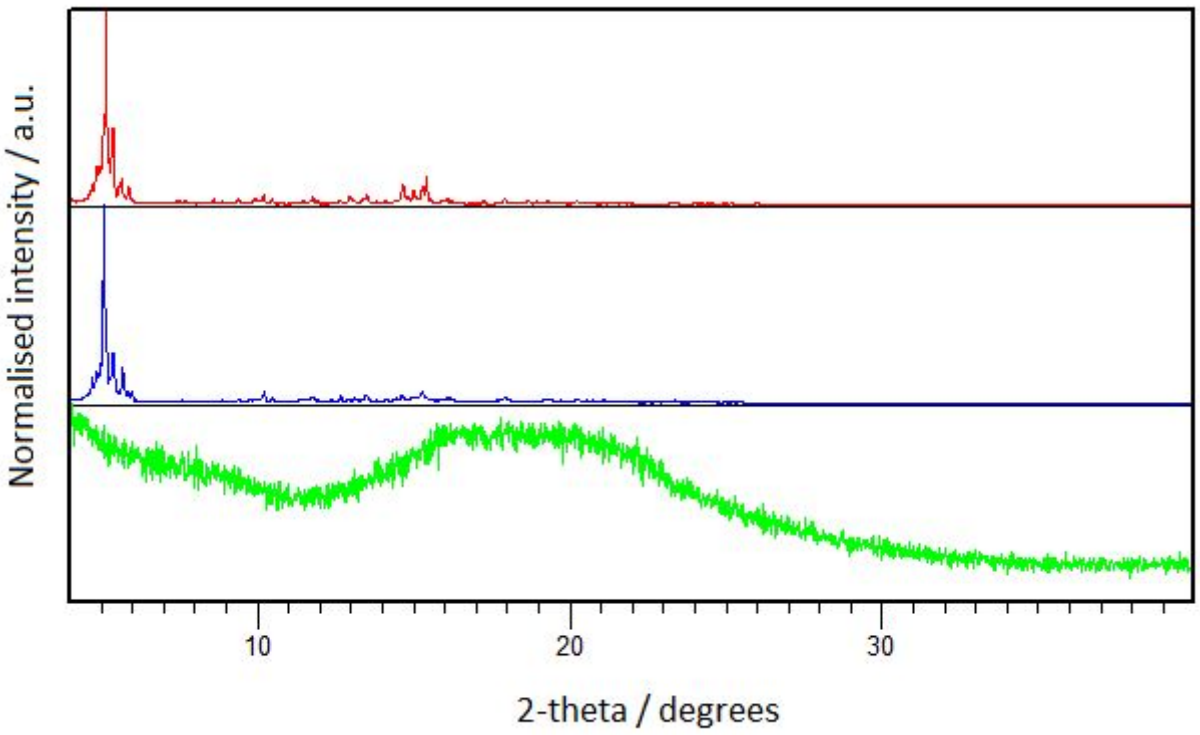

Figure S13. PXRD patterns recorded after drying the *n*-pentane solvated *Im*$\bar{3}$ **CC20** phase in air (humidity 28–31%) for 30 minutes (red, top), 1 day (blue, middle), and 2 days (green, bottom).

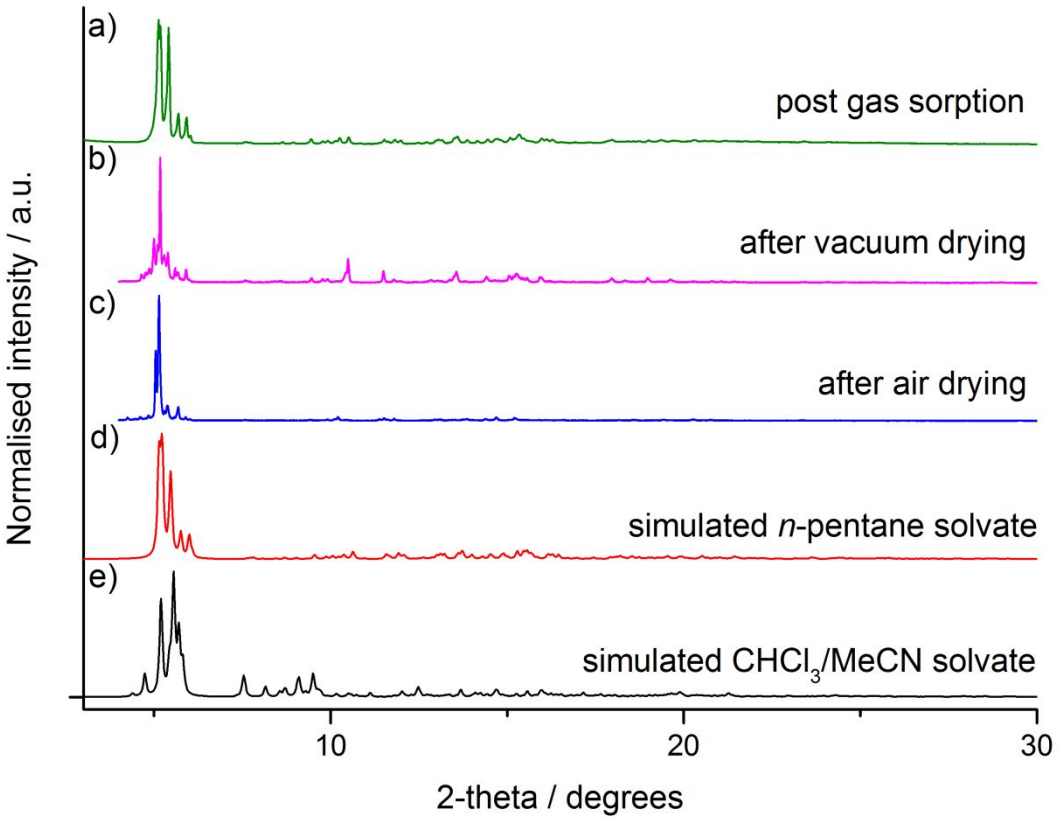

Figure S14. PXRD patterns recorded after activating the *n*-pentane solvated $P\bar{1}$ **CC20** phase and recording gas sorption isotherms. PXRD patterns recorded; (a) post gas sorption analysis, (b) after drying the *n*-pentane solvated crystals at 30 °C under vacuum for 3 days, and (c) after drying the *n*-pentane solvated crystal in air at ambient temperature. Simulated PXRD patterns of the *n*-pentane (d) and $CHCl_3$/MeCN (e) **CC20** $P\bar{1}$ solvates.

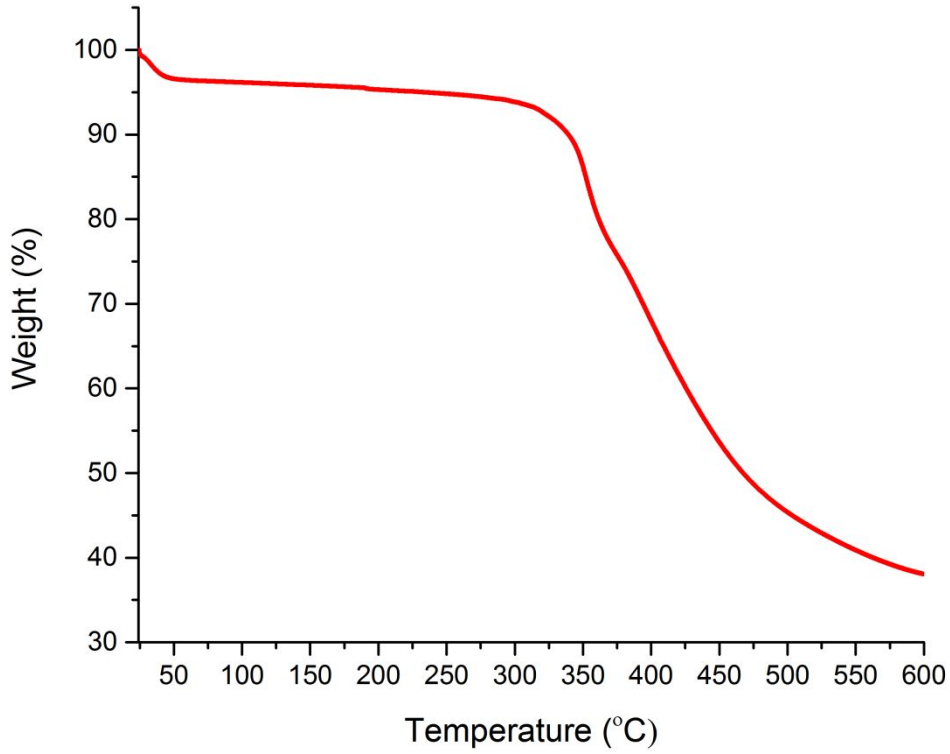

Figure S15. Thermogravimetric analysis (TGA) for **CC20** $P\bar{1}$ phase, recording after degassing the *n*-pentane $P\bar{1}$ **CC20** solvate at 30 °C. TGA recorded under a N_2 gas flow with a heating rate 10 °C/min.

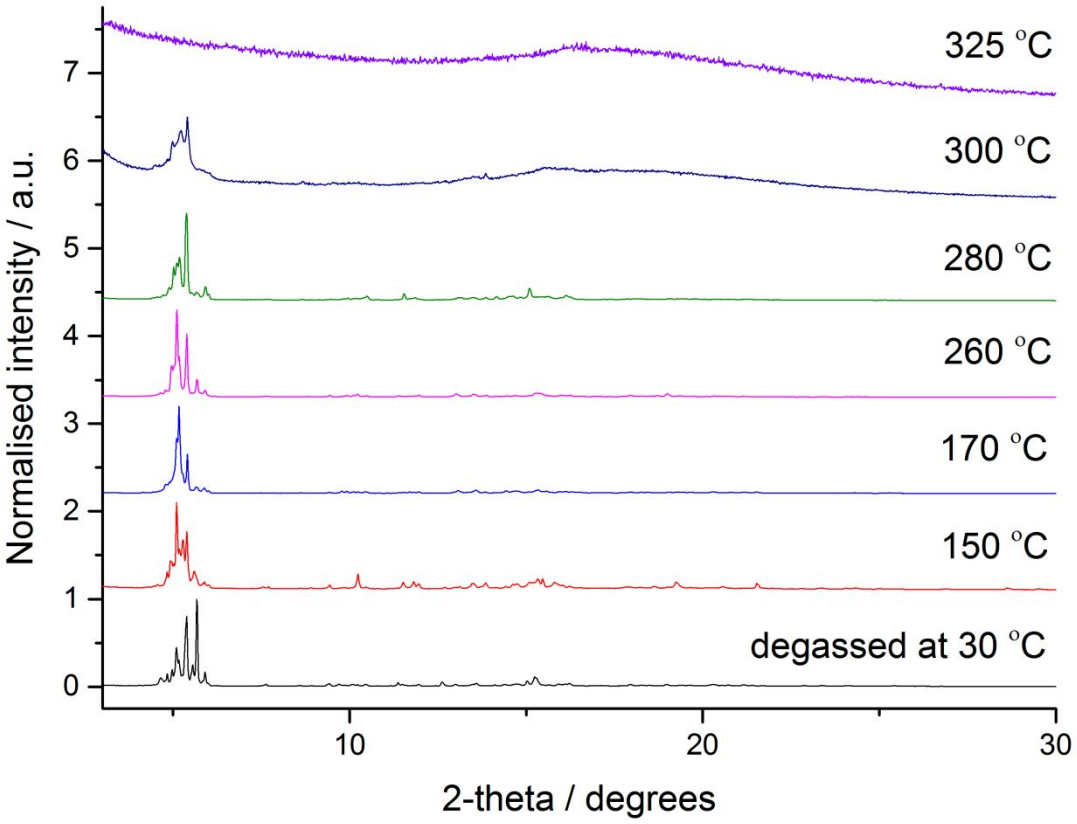

Figure S16. Variable temperature PXRD patterns for the degassed $P\bar{1}$ phase, recording after degassing the *n*-pentane $P\bar{1}$ **CC20** solvate at 30 °C. The PXRD patterns were recorded after heating samples of this phase to 150, 170, 260, 280, 300 and 325 °C for 30 minutes under a N_2 gas flow. All PXRD patterns were recorded at room temperature after cooling the samples to RT under N_2. The loss of crystallinity correlates with the onset of weight loss in the TGA plot.

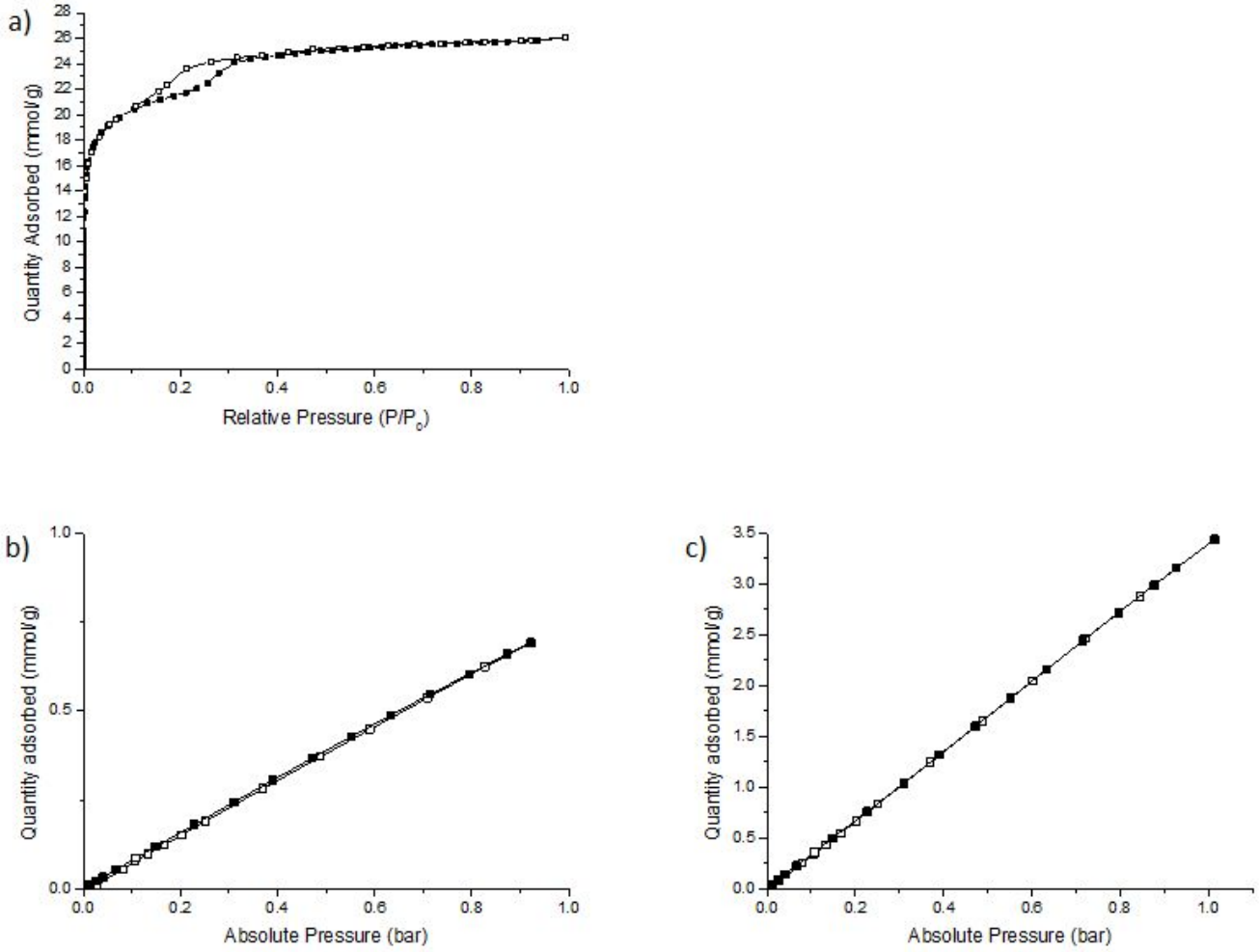

Figure S17. Gas sorption isotherms recorded for the **CC20** material that was initially crystallised from $CHCl_3$/MeCN, then solvent exchanged with *n*-pentane, before being degassed for 15 hours under vacuum at 30 °C. a) N_2 sorption isotherms at 77.3 K, b) Kr sorption isotherm at 273 K, and c) Xe sorption isotherm at 273 K (closed symbols for adsorption, open for desorption).

Table S18. Summary of gas sorption data for **CC20**

[a]SA_{BET} was calculated from the N_2 isotherm in the relative pressure (P/P_0) range 0.0 to 0.10.

	SA_{BET} (m^2g^{-1}, N_2 at 77 K)	Uptake of Gases at 1 bar (mmol g^{-1})				
		N_2 (at 77 K)	H_2 (at 77 K)	CO_2 (273 K)	Xe (273 K)	Kr (273 K)
CC20 DCM/MeOH phase	5[a]	0.35	2.10	-	-	-
CC20 *n*-Pentane phase	829[a]	15.79	-	1.69	1.81	0.43
CC20 $CHCl_3$/MeCN phase	1752[a]	26.06	-	-	3.44	0.69

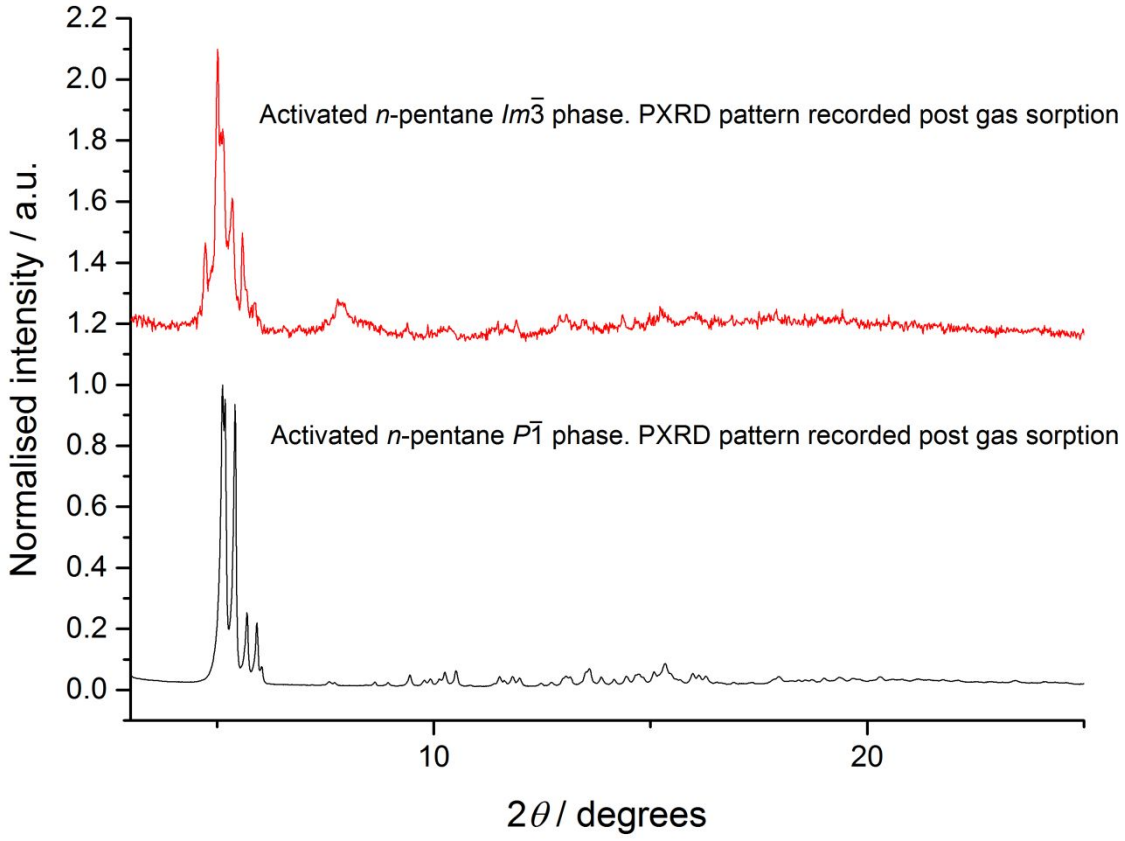

Figure S19. Comparison between PXRD patterns recorded after activating the *n*-pentane solvated $Im\bar{3}$ phase and recording gas sorption isotherms (top), and after activating *n*-pentane solvated $P\bar{1}$ phase and recording gas sorption isotherms (bottom).

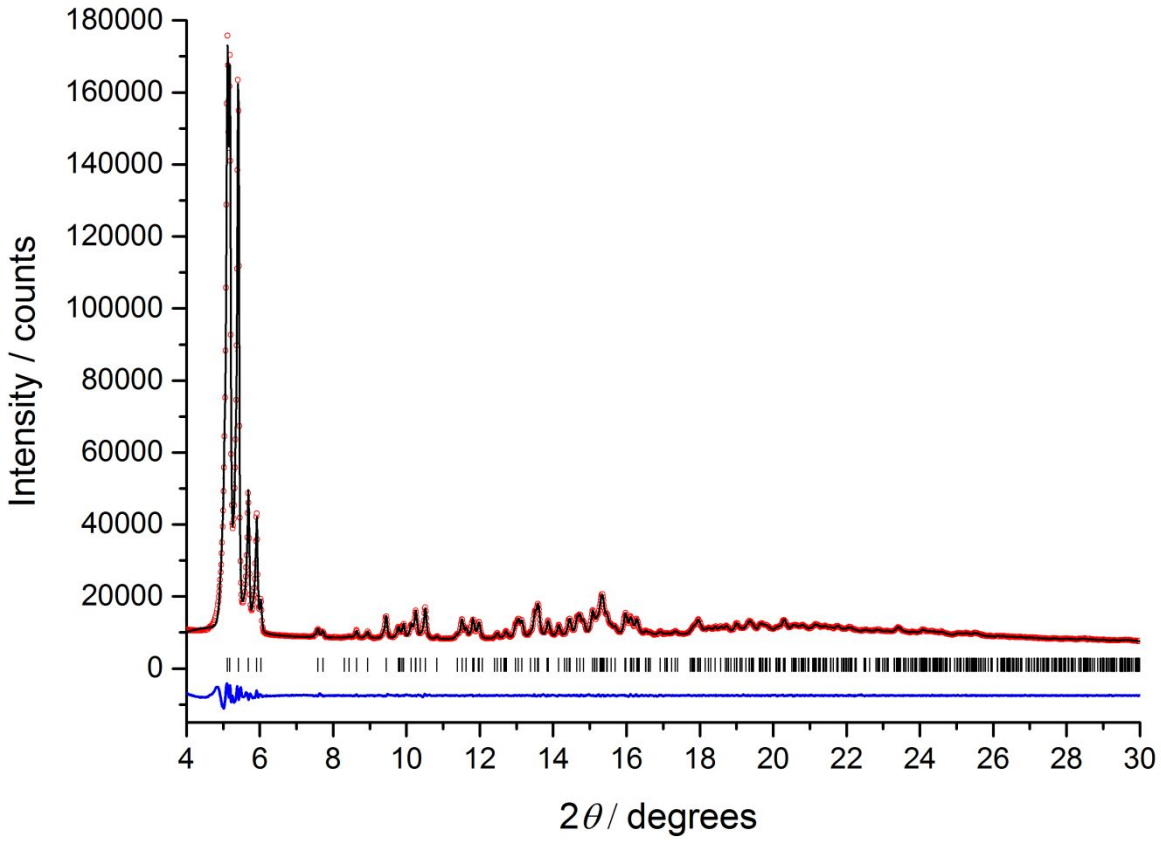

Figure S20. Le Bail fit for $P\bar{1}$ **CC20** phase, recorded after activation and measuring gas sorption isotherms; final observed (*red*), calculated (*black*) and difference (*blue*) PXRD profiles for Le Bail refinement (R_{wp} = 2.97%, R_p = 1.93%, χ^2 = 2.48, a = 18.552(1) Å, b = 18.894(1) Å, c = 19.339(1) Å; α = 103.196(3)°, β = 119.007(6)°, γ = 103.6444(4)°; V = 5806.9(7) Å^3). This measurement was performed using a sample loaded in a borosilicate glass capillary. The volume of this Le Bail fitted unit cell is ~50% of the unit cell volume of the *n*-pentane solvated $P\bar{1}$ phase (V = 11278.9(7) Å^3).

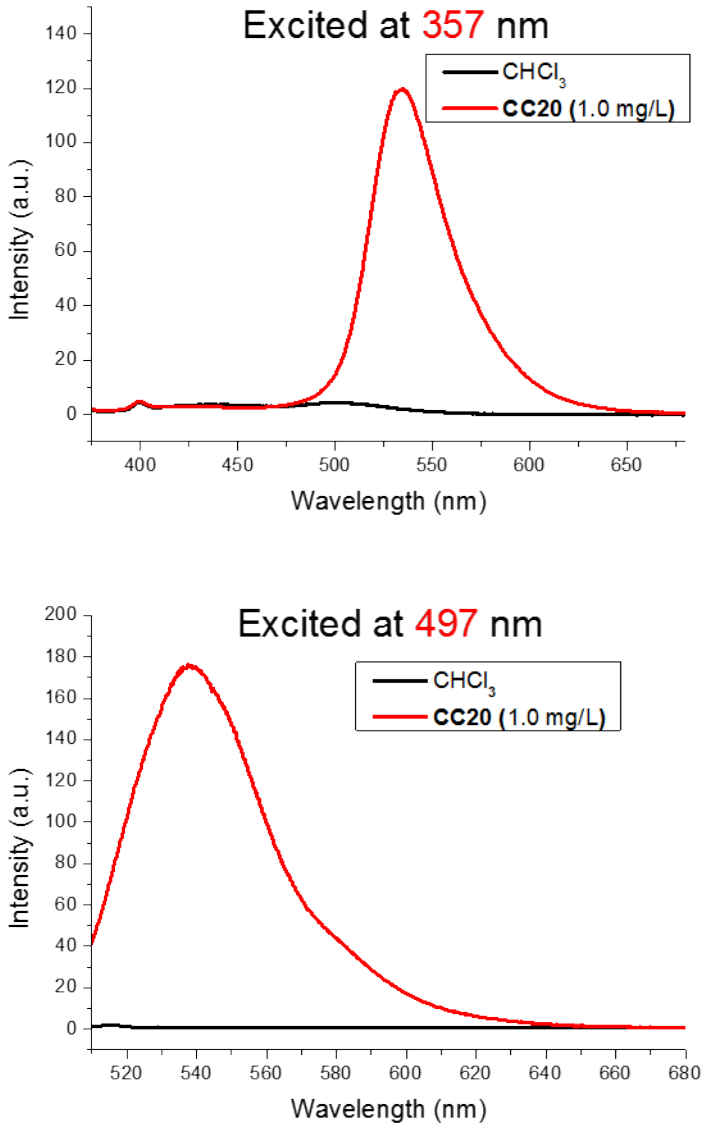

Figure S21. Fluorescence emission spectra of **CC20** in $CHCl_3$ at 357 (top) and 497 nm (bottom). Both excitation wavelengths give emission at 534 nm (yellow-green colour).

Figure S22. Fluorescence emission of a chloroform solution of **CC20** under irradiation with UV light (365 nm).

Addition refinement details:

The four single crystal structures of **CC20** were disordered and weakly diffracting. As a result, it was not possible to model all the solvent molecules in the large lattice voids during refinement. Therefore, it was necessary to use the SQUEEZE routine in Platon during the final refinement cycles of all the **CC20** crystal structures in this study.[11,12] For displacement ellipsoids plots from the single crystal structures, see **Figures S20-21**.

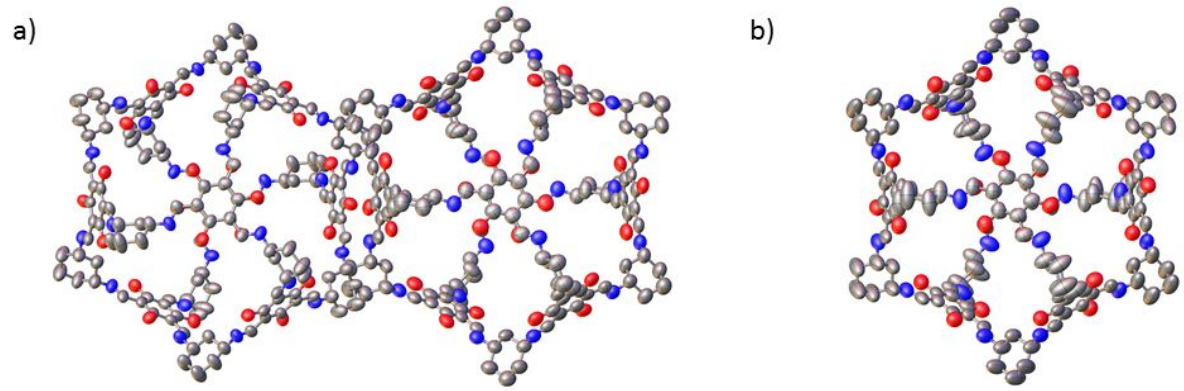

Figure 23. Displacement ellipsoid plots from the single crystal structures 2(**CC20**)·46(CH_2Cl_2)·46(CH_4O) (a) and (**CC20**)·32(C_5H_{12}) (b) recorded at 100 K. Ellipsoids shown at 20% probability level; **CC20** molecules shown in entirety; -OH groups are disordered in the crystal structures; H-atoms omitted for clarity.

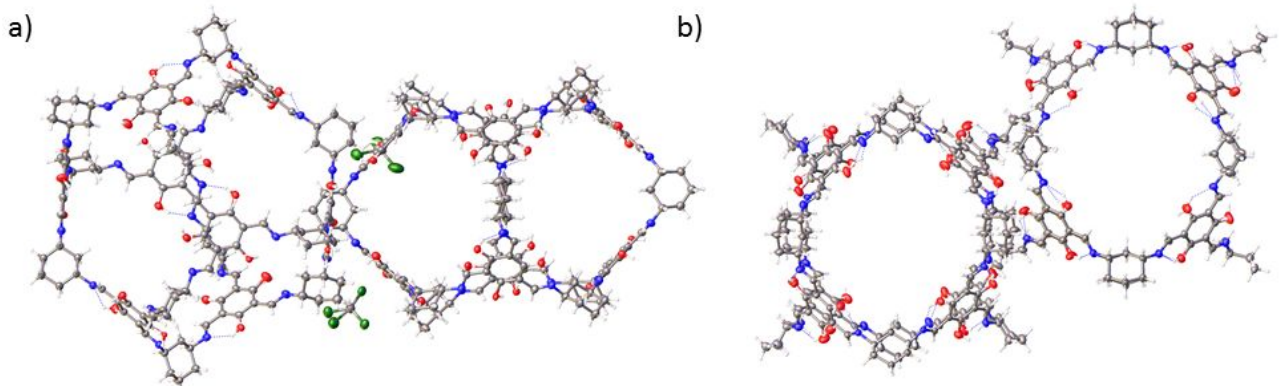

Figure 24. Displacement ellipsoid plots from the single crystal structures 2(**CC20**)·26($CHCl_3$)·23(C_2H_3N) (a), and 2(**CC20**)·17.5(C_5H_{12}) (b), recorded at 100 K. Ellipsoids shown at 20% probability level, **CC20** molecules shown in entirety; -OH groups are disordered in the crystal structures.

Supplementary References

(1) Jorgensen, W. L.; Maxwell, D. S.; Tirado-Rives, J. Development and Testing of the OPLS All-Atom Force Field on Conformational Energetics and Properties of Organic Liquids. *J. Am. Chem. Soc.* **1996**.

(2) Santolini, V.; Tribello, G. A.; Jelfs, K. E. Predicting Solvent Effects on the Structure of Porous Organic Molecules. *Chem. Commun.* **2015**, *51*, 15542–15545.

(3) Parsons, S. ECLIPSE. The Univeristy of Edinburgh, Edinburgh, UK 2004.

(4) Sheldrick, G. M. SADABS. Program for Empirical Absorption Correction. University of Gottingen, Germany 2008.

(5) Krause, L.; Herbst-Irmer, R.; Sheldrick, G. M.; Stalke, D. Comparison of Silver and Molybdenum Microfocus X-Ray Sources for Single-Crystal Structure Determination. *J. Appl. Crystallogr.* **2015**, *48*, 3–10.

(6) Sheldrick, G. M. Experimental Phasing with SHELXC/D/E: Combining Chain Tracing with Density Modification. *Acta Crystallogr. Sect. D Biol. Crystallogr.* **2010**, *66*, 479–485.

(7) Sheldrick, G. M. SHELXT - Integrated Space-Group and Crystal-Structure Determination. *Acta Crystallogr. Sect. A Found. Crystallogr.* **2015**, *71*, 3–8.

(8) Sheldrick, G. M. A Short History of SHELX. *Acta Crystallographica Section A: Foundations of Crystallography*. American Association for the Advancement of Science January 1, 2008, 112–122.

(9) Sheldrick, G. M. Crystal Structure Refinement with *SHELXL*. *Acta Crystallogr. Sect. C Struct. Chem.* **2015**, *71*, 3–8.

(10) Dolomanov, O. V.; Bourhis, L. J.; Gildea, R. J.; Howard, J. A. K.; Puschmann, H. *OLEX2* : A Complete Structure Solution, Refinement and Analysis Program. *J. Appl. Crystallogr.* **2009**, *42*, 339–341.

(11) Spek, A., PLATON, An Integrated Tool for the Analysis of the Results of a Single Crystal Structure Determination. *Acta Cryst. Sect. A* **1990**, *46*, c34.

(12) Van Der Sluis, P.; Spek, A. L., BYPASS: an effective method for the refinement of crystal structures containing disordered solvent regions. *Acta Cryst. Sect. A* **1990**, *46*, 194-201.